

IMPACT OF HEXADECAPOLE DEFORMATION ON FUSION CROSS SECTIONS OF SOME SPHERICAL + DEFORMED SYSTEMS IN 3S-CMD MODEL

 Jignasha Patel^{1*},  Vipul Katariya²

¹*Veer Narmad South Gujarat University, Surat - 395007, Gujarat, INDIA*

²*Department of Physics, Atmanand Saraswati Science College, Surat - 395006, Gujarat, INDIA*

*Corresponding Author e-mail: pateljignasha87@gmail.com

Received October 28, 2025; revised December 17, 2025, accepted January 8, 2026

The effect of quadrupole deformation (β_2) on heavy ion fusion is a fact that is well recognized phenomenon. In addition to the influence of quadrupole deformation (β_2), the potential impact of hexadecapole deformation (β_4) on sub-barrier fusion has been a topic of frequent discussion. Recently, a theoretical analysis was performed to examine the impact of hexadecapole deformations (β_4), employing the simplified coupled channels code CCFUS, which incorporates static deformations. In this study, we analyze the effect of the β_4 of the target nucleus on fusion cross sections within the framework of the 3S-CMD model. For this purpose, we have chosen the reactions $^{16}\text{O} + ^{154}\text{Sm}$ and $^{16}\text{O} + ^{174}\text{Yb}$. The present research has calculated the fusion cross sections using the SBPM model as well. The calculated fusion cross sections using 3S-CMD model and SBPM are compared with each other as well as experiment.

Keywords: *Deformed nuclei; Quadrupole; Hexadecapole; Fusion cross sections; Classical microscopic approaches; Heavy-ion reactions*

PACS: 24.10.-i; 25.70.De; 25.60.Pj

1. INTRODUCTION

The study of hexadecapole deformation (β_4) of deformed body is essential for understanding the creation of superheavy elements (SHEs). Thus, the deformation associated with the hexadecapole may considerably modify the height of the fusion barrier. This consequently affects the fusion probability and, as a result, the likelihood of superheavy elements (SHEs) [1] formation. Theoretically, it has been proposed that a hexadecapole deformation (β_4) could facilitate fusion, resulting in the formation of superheavy elements (SHEs), depending on the chosen reaction partners [2]. Moreover, it is expected that hexadecapole deformation (β_4) will have a meaningful impact on the fusion process. The fusion barrier distributions derived from experimental findings demonstrate that fusion reactions are notably influenced by quadrupole deformation (β_2) and even by minor adjustments in hexadecapole deformation (β_4) [3].

Recently, a theoretical analysis focused on the importance of hexadecapole deformation (β_4) was performed using the simplified coupled channels code CCFUS, which incorporates static deformations. The predictions highlight considerable changes in the fusion cross sections. Positive values of β_4 are expected to enhance fusion while negative values will decrease it with respect to the $\beta_4 = 0$ system [4, 5].

The process of experimentally obtaining hexadecapole deformation (β_4) is challenging, with results that depend heavily on the chosen models and considerably vary with significant inaccuracies. Conceptually, the method that combines macroscopic and microscopic perspectives [6, 7] has been utilized to compute the deformation of nuclei in their ground state. In the present work, we modify the “STATIC” code [8] to calculate hexadecapole deformation (β_4). The hexadecapole deformation and the other ground-state properties are calculated using this code. By using the obtained ground-state properties, fusion cross sections have been calculated in 3S-CMD [9] and SBPM [9] model. During the approach stage of a heavy-ion collision, the higher deformation (in this study hexadecapole deformation) of the nucleus near the fusion barrier changes the barrier parameters, which in turn affect fusion cross-section calculations. Therefore, the effect of deformation on fusion cross-section calculation is studied for Spherical + Deformed systems and is discussed in detail in this article.

The motivation of this study is to find the impact of hexadecapole deformation of various target nuclei keeping the projectile nucleus same on fusion cross sections in 3S-CMD model. Fusion cross sections have been calculated for $^{16}\text{O} + ^{154}\text{Sm}$ and $^{16}\text{O} + ^{174}\text{Yb}$ systems. As long as the doubly magic ^{16}O nucleus is thought of to be spherical, it is expected that any effects of nuclear shapes on fusion cross sections will arise solely from the target nuclei.

The structure of this study is outlined as follows: Section 2 contains calculation details which include calculation of NN-potential, construction of the nuclei in ground state, evaluation of fusion cross sections together with a brief summary of the models which is used to find fusion cross sections. Section 3 provides a summary of the results obtained through the dynamic simulation. The final section gives the conclusion of the findings.

2. CALCULATION DETAILS

2.1. Nucleon-Nucleon potential

The NN potential utilized in this research is a soft-core Gaussian potential, which is entirely phenomenological and can be described by the following equation [10],

$$V_N(r_{ij}) = -V_0 \left(1 - \frac{C}{r_{ij}}\right) \exp\left(-\frac{r_{ij}^2}{r_0^2}\right), \quad (1)$$

where, V_0 , C and r_0 are respectively, the depth parameter, repulsive-core radius and range parameter. The parameters V_0 , C and r_0 are chosen so that the NN-potential reproduces gross characteristics of the nuclei in their ground state such as the ground state binding energy, the rms radius etc.

The Coulomb potential between protons

$$V_C(r_{ij}) = \frac{1.44}{r_{ij}} (\text{MeV}), \quad (2)$$

is also added to the nuclear potential.

2.2. Construction of nuclei in their ground state

Nuclei in the ground state are generated through the “STATIC” procedure, which starts with a random distribution of nucleon positions within a defined spherical radius. Subsequently, the total potential energy of these nucleon configurations is minimized cyclically by making slight displacements to the coordinates of each nucleon.

Total BE is the total potential energy and R_{rms} is calculated from all the nucleon positions. The quadrupole deformation parameter (β_2) is calculated from the expression [11],

$$\beta_2 = \sqrt{\frac{16\pi}{5}} \left(1 - \frac{R(90^\circ)}{R_0}\right), \quad (3)$$

where, $R(90^\circ)$ is the length of the two equal axes perpendicular to the symmetry axis and R_{rms} is the rms radius of the spherical nucleus.

For the given nucleus if its symmetry axis is greater than R_{rms} , $R(90^\circ) < R_{\text{rms}}$ in eq. (3) and hence the β_2 of that nucleus is positive (prolate deformation). Similarly, if the symmetry axis of the given nucleus is less than R_{rms} , $R(90^\circ) > R_{\text{rms}}$ in eq. (3) and hence the β_2 of that nucleus is negative (oblate deformation).

The hexadecapole deformation parameter (β_4) is calculated from the expression

$$\beta_4 = \left(\frac{16}{9}\sqrt{\pi}\right) \left[\frac{R(90)}{R_0} - 1 + \beta_2 \left(\sqrt{\frac{5}{16\pi}}\right)\right], \quad (4)$$

in terms of rms radius of the nucleus and $R(90^\circ)$ which is the length of the axes along the direction of any one of the principal axes perpendicular to the symmetry axis.

The ultimate configuration of nucleon placements leads to a stable nucleus. Considering that for $A \geq 5$, there may be multiple local minima in the binding energy, a nucleus is chosen that demonstrates the highest binding energy from a diverse range of configurations (the most-bound nucleus) [12]. Alternatively, a configuration that bears a strong resemblance to the properties of the experimental ground state is chosen [13].

A parameter set $V_0 = 1155$ MeV, $C = 2.07$ fm, $r_0 = 1.2$ fm is used in the present calculation which produces the ground state characteristics of the colliding nuclei is shown in Table 1.

Table 1. The characteristics of the produced nuclei in their ground state.

	Calculated				Experimental			
	B.E. (Mev)	RMS (fm)	β_2	β_4	B.E. (Mev)	RMS (fm)	β_2	β_4
^{16}O	-125.36	2.47	0.15	-0.08	-127.62	2.73	0.00	-0.12
^{154}Sm	-1375.86	5.46	0.20	-0.11	-1266.94	5.12	0.27	0.10
^{174}Yb	-1478.90	5.71	0.12	-0.06	-1406.60	5.41	0.28	-0.05

Fig. 1 shows the ground state characteristics of all the configurations of the ^{16}O , ^{154}Sm and ^{174}Yb nuclei generated by the “STATIC” method. Among the large set of generated configurations for the nuclei, those that exhibit ground state properties closely aligned with experimental values are chosen for collision calculations. These systems are indicated by bigger open circle and triangle in Fig. 1.

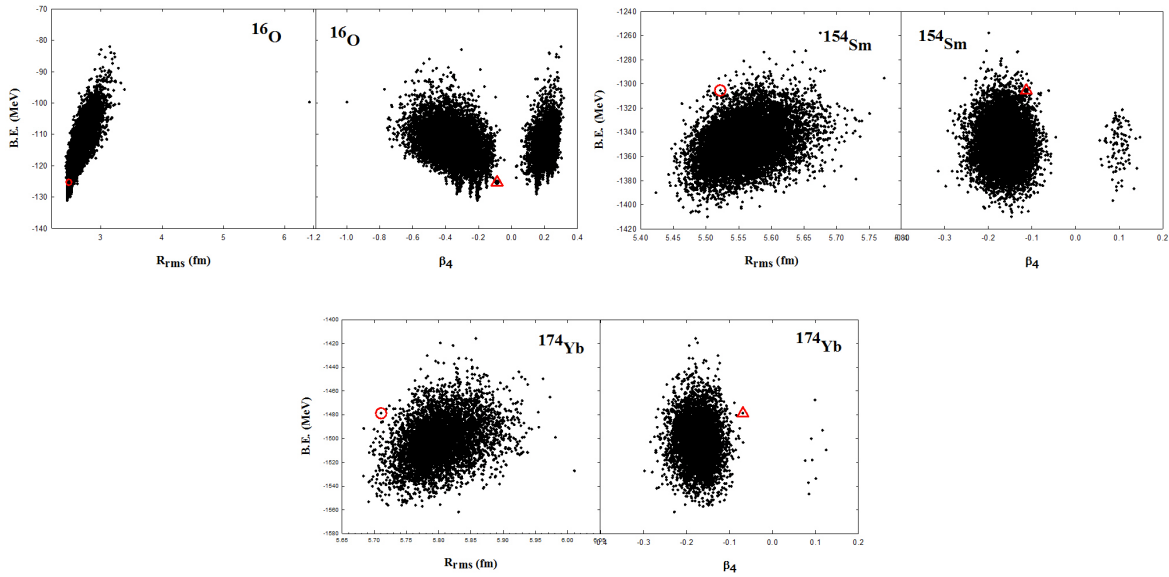


Figure 1. Ground state characteristics of the ^{16}O , ^{154}Sm and ^{174}Yb nuclei generated by the “STATIC” method. \circ and \triangle indicate the ground state characteristics of the nuclei used in the present study.

2.3. Analysis of fusion cross sections involving hexadecapole deformation

Calculations of fusion cross sections have been performed for numerous reactions that involve nuclei displaying various collective degrees of freedom. Different models have been employed to calculate the fusion cross sections, such as Time Dependent Hartree Fock (TDHF) [14, 15], classical trajectory methods [16], and the coupled channel calculation software referred to as CCFULL [17]. However, methods based on quantum mechanics at the microscopic scale, such as TDHF calculations, are very compute-intensive, and CCFULL calculations, which are static, do not reflect the effects of dynamical reorientation.

The barrier parameters at $b = 0$ (indicating a head-on collision) which corresponds to a specific collision energy and the initial orientation of the two nuclei, are derived from a dynamically generated ion-ion potential. With these parameters, fusion cross-section is calculated using Wong’s formula [18],

$$\sigma_{\text{fus}}(E_{\text{CM}}) = \left[\frac{R_B^2 \hbar \omega_0}{2E_{\text{CM}}} \right] \ln \left\{ 1 + \exp \left(2\pi \frac{E_{\text{CM}} - V_B}{\hbar \omega_0} \right) \right\}, \quad (5)$$

where V_B denotes the height of the barrier, R_B represents the radius of the barrier, and ω_0 signifies the oscillator frequency associated with the peak of the barrier. The method used to find barrier parameters affects the fusion cross-sections.

The calculations of heavy-ion fusion cross sections have been performed using SBPM and 3S-CMD methods within the context of classical approximations. $^{16}\text{O} + ^{154}\text{Sm}$ and $^{16}\text{O} + ^{174}\text{Yb}$ reaction has been studied in this approach with the potential parameter set P4 ($V_0 = 1155$ MeV, $C = 2.07$ fm and $r_0 = 1.2$ fm). The $^{16}\text{O} + ^{154}\text{Sm}$ system has been well studied in SBPM model in ref. [10] and in CRBD model in ref. [11] using the same NN potential parameter set P4.

2.4. Model Details

- **SBPM Model :** The ion-ion potential is formulated as a function of the center of mass separation (R_{CM}) of the two nuclei, as derived from the impulse approximation (i.e., keeping the configuration of the nucleons in the two nuclei frozen during their collision) [9]. The ion-ion potential consists of the total nuclear and Coulomb potentials that exist between all nucleons of the two ions. The parameters V_B and R_B represent the outer maximum of the ion-ion potential, while ω_B denotes the second derivative of this peak. This gives barrier parameters of head-on collision for a given orientation of the two nuclei. Large numbers of such randomly chosen orientations of the two nuclei are considered in this study. All the degree of freedom are explicitly neglected in this model.
- **3S-CMD Model :** The simulation of heavy-ion collisions within the present classical approach (3S-CMD) occurs in three sequential stages:
 - (1) **Rutherford Trajectory Calculation:** The two nuclei, treated as charged point particles, are directed along their Rutherford trajectories with a defined collision energy (E_{CM}) and impact parameter (b) until they attain a separation of $R_{\text{CM}} = 2500$ fm.

(2) CRBD model Calculation: The two nuclei, considered as rigid bodies with a fixed arrangement of nucleon positions in their ground state, are subsequently permitted to evolve further through the CRBD model [19]. This is achieved by solving the translational and rotational equations of motion for their center of mass and the orientation angles of their principal axes. The process of CRBD calculation is carried on until a relatively small separation of $R_{CM} = 50$ fm is attained.

(3) CMD Calculation: The Rigid body constraints are relaxed at approximately $R_{CM} = 50$ fm, and the paths of all the participating nucleons are calculated using the coupled Newton's equations of motion for each particle within a CMD framework [20].

3. RESULT AND DISCUSSION

$^{16}\text{O} + ^{154}\text{Sm}$: The $^{16}\text{O} + ^{154}\text{Sm}$ system has been selected to investigate the impact of hexadecapole deformation, as it has been extensively examined through both experimental [21] and theoretical approaches [10, 11]. The phase of the collision as it approaches the barrier top is influenced by the center-of-mass energy, E_{CM} . Because barrier parameters are the key components in fusion cross-section calculations, a detailed understanding of the variations in the ion-ion potential V_{12} and the barrier parameters with respect to the collision energy E_{CM} is required.

Fig. 2 illustrates the ion-ion potential for the $^{16}\text{O} + ^{154}\text{Sm}$ system, calculated with an initial $R_{in} = 2500$ fm across various collision energies (E_{CM}), while maintaining the same arbitrary initial orientation for each case. This figure illustrates that both the barrier height V_B and the barrier radius R_B are influenced by the incident energy E_{CM} . Thus, it is essential to determine the barrier parameters (V_B , R_B , ω_0) based on a specified initial orientation and a defined collision energy. To determine the fusion cross section, it is essential to take the average of the barrier parameters across numerous initial random orientations. The fusion cross-section obtained is specific to the fusion cross-section at that particular collision energy only.

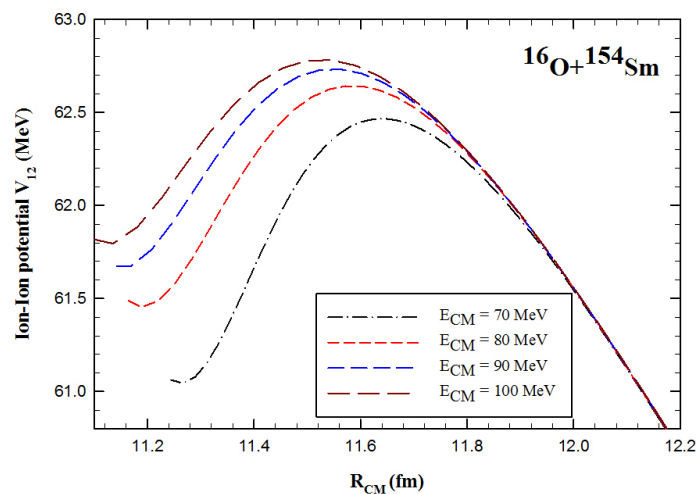


Figure 2. Ion-ion potential V_{12} as a function of center-of-mass separation R_{CM} for $^{16}\text{O} + ^{154}\text{Sm}$ system for different collision energy E_{CM} but same arbitrary orientation.

The fusion cross-section of the $^{16}\text{O} + ^{154}\text{Sm}$ system is calculated in SBPM calculations, utilizing the NN potential parameter set P4 ($V_0 = 1155$ MeV, $C = 2.07$ fm and $r_0 = 1.2$ fm) shown in Fig. 3. This figure also shows the fusion cross sections calculated for $^{16}\text{O} + ^{154}\text{Sm}$ system in 3S-CMD model with the same potential parameter set along with the experimental data of ref. [21]. Fusion cross-section are calculated for $^{16}\text{O} + ^{154}\text{Sm}$ system in 3S-CMD model for central collisions ($b = 0$). The ^{16}O and ^{154}Sm nucleus are dynamically evolved as a rigid body till the target-projectile separation is close to their barrier top (about 13 fm). At this separation the rigid body constraint on both the ^{16}O and ^{154}Sm are relaxed for further evolution of the entire system. Comparison of fusion cross sections calculated by considering the quadrupole deformation and hexadecapole deformation using both the models is also shown in Fig. 3.

It is evident from Fig. 3 that the fusion cross sections calculated for quadrupole deformation and hexadecapole deformation in the SBPM model agrees well with the experimental data as well as with each other at higher energy levels. At lower energy levels, the SBPM calculations tend to overestimate the experimental fusion cross-sections for both the deformations. Fusion cross sections calculated for the hexadecapole deformations are highly overestimated with the experimental data whereas fusion cross sections calculated for the quadrupole deformations are slightly overestimated with the experimental data at lower energy side. Fusion cross sections calculated for quadrupole deformation and hexadecapole deformation in 3S-CMD model are highly overestimated with the experimental data at all energy levels. At lower energy

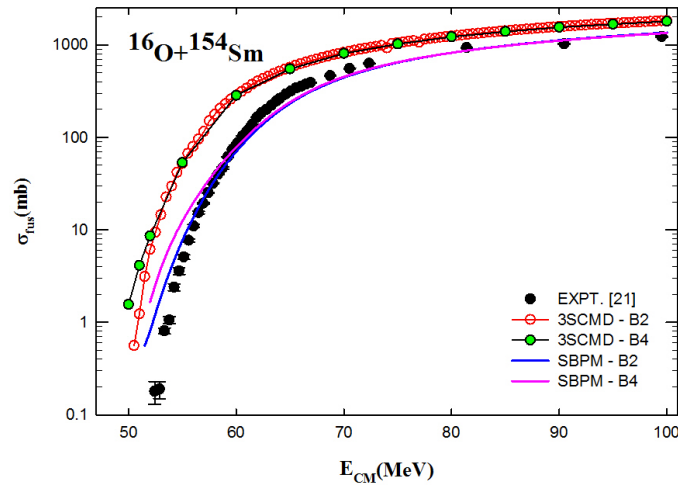


Figure 3. Comparison of fusion cross sections calculated for quadrupole and hexadecapole deformation using SBPM and 3S-CMD model with experimental fusion cross sections for $^{16}\text{O} + ^{154}\text{Sm}$ system.

side, the fusion cross section calculated quadrupole deformation and hexadecapole deformation in 3S-CMD model shows same trend as in SBPM calculation.

At low collision energy levels, the duration of interaction between the colliding nuclei becomes longer. This causes the reorientation of the deformed ^{154}Sm in relation to the spherical ^{16}O nucleus. However, the extent of reorientation is small because the target nucleus (^{154}Sm) is medium heavy and has large moment of inertia. As mentioned in ref. [11], at lower energy the fusion cross sections calculated using CRBD model and SBPM model shows small difference. Because the CRBD model only considered rotational degree of freedom. This research calculates the fusion cross sections through the 3S-CMD model, which incorporates both the long-range rotational excitation (reorientation effect) and the vibrational excitations that occur in proximity to or within the barrier and this could be one of the reason in difference of fusion cross sections between SBPM and 3S-CMD model.

Additionally, the fusion cross sections calculated using 3S-CMD model overestimated at all energies with the experimental fusion cross sections. In order to examine this anomaly, we carry out an examination of the ground state properties of the nuclei involved in the above calculations. Ground state properties of the nuclei used in present calculation are shown in the Table 1.

From the Table 1, it is noted that experimentally determined values of β_2 indicate that ^{16}O is spherical while the ^{16}O nucleus generated in present study is being prolate ($\beta_2 = 0.157$). The experimental β_4 value for ^{154}Sm is positive while the calculated β_4 value is negative. Calculated rms radius of ^{16}O nucleus is found to be smaller than the experimental rms value by about 10 % while that for ^{154}Sm is larger by about 6 %. Thus, the smaller dimensions of the lighter nucleus, when combined with the larger dimensions of the heavier nucleus, contribute to an overestimation of the fusion cross sections for this particular reaction.

T_{rot} for non-rigid case with $E_{\text{CM}} = 100$ MeV and $b = 0$ fm are shown in Fig. 4. At $b = 0$ fm, T_{rot} is higher initially but soon it reduces to very low values because for central collision $T_{\text{rot}}(^{16}\text{O})$ and $T_{\text{rot}}(^{154}\text{Sm})$ dissipates very soon as shown in Fig. 4. The light prolate ^{16}O acquire comparatively high T_{rot} initially on the contact with the heavy-medium deformed ^{154}Sm but it dissipates soon to very low level.

Fig. 5 shows the total vibrational excitation energy (T_{vib}) of $^{16}\text{O} + ^{154}\text{Sm}$ system at $b = 0.0$ fm. From the Fig. 4 and Fig. 5 we can see that for the central collision ^{154}Sm acquire a small T_{rot} but large T_{vib} resulting from the maximum change in the internal potential energy (binding energy) of the ^{154}Sm .

$^{16}\text{O} + ^{174}\text{Yb}$: In order to clearly bring out the effect of hexadecapole deformation on fusion cross sections, we replace the medium-heavy target nucleus (^{154}Sm) with heavy nucleus (^{174}Yb) with same projectile (^{16}O). In this system both the projectile and target nuclei having prolate quadrupole deformation with $\beta_2 = +0.157$ (^{16}O) and $\beta_2 = +0.123$ (^{174}Yb). For $^{16}\text{O} + ^{174}\text{Yb}$ system, the mass asymmetry between ^{16}O and ^{174}Yb is somewhat greater than that observed between ^{16}O and ^{154}Sm . The ground state configuration of generated nuclei are shown in Fig. 1 and the ground state properties of the generated nuclei are shown in Table 1. From the Table 1, it has been observed that the binding energy and rms radius of ^{174}Yb nucleus are overestimate by 5% where as quadrupole deformation parameter β_2 is reduced by 1%. The experimental and calculated β_4 value is negative for both the projectile and target nuclei.

Fusion cross-sections for $^{16}\text{O} + ^{174}\text{Yb}$ system is calculated using SBPM and 3S-CMD model are shown in Fig. 6. From this figure it is clear that the fusion cross sections calculated using SBPM model with quadrupole and hexadecapole deformation shows good agreement at higher energies with the experimental data while below the barrier energies it

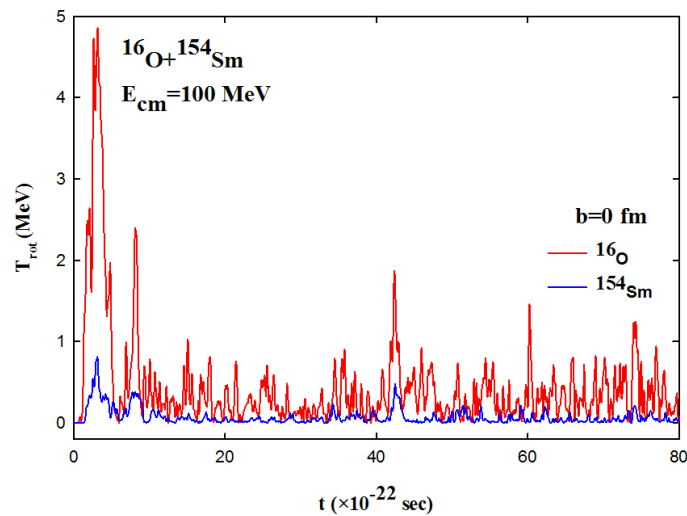


Figure 4. Total rotational kinetic energy (T_{rot}) of $^{16}\text{O} + ^{154}\text{Sm}$ system at $b = 0.0$ fm.

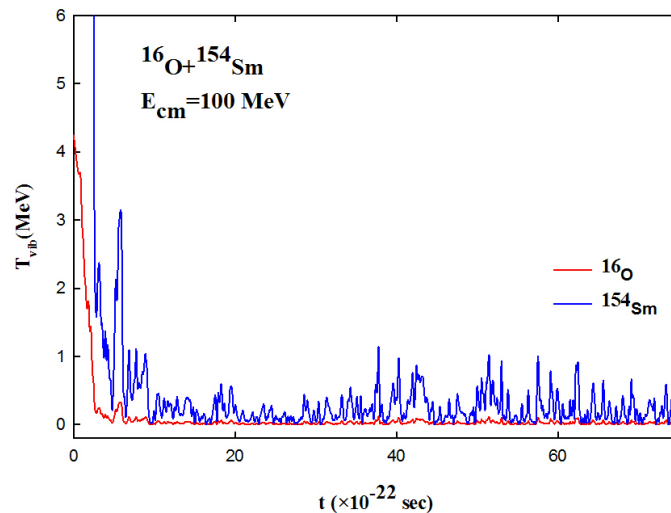


Figure 5. Total vibrational excitation energy (T_{vib}) of $^{16}\text{O} + ^{154}\text{Sm}$ system at $b = 0.0$ fm.

over estimates the experiment. The result of fusion cross sections calculated using 3S-CMD model with quadrupole and hexadecapole deformation are close to the experiment at higher energies. At sub-barrier energies, the fusion cross sections calculated using 3S-CMD model with both the deformations are highly overestimated.

The fusion cross sections corresponding to a particular collision energy in the 3S-CMD calculation are derived by averaging the orientations of the fusion cross sections determined through Wong's formula, utilizing barrier parameters specific to that energy simulation. About 500 initial random orientation were considered for $E_{CM} \geq 80$ MeV and 1000 for $E_{CM} < 80$ MeV.

As the reorientation and vibrational effects are likely to be prominent at collision energies near the Coulomb barrier, it is essential to investigate fusion cross-sections at energy levels that are significantly below the lowest E_{CM} indicated in ref. [14]. To effectively highlight both the effect of reorientation + vibration, fusion cross-sections are calculated in 3S-CMD for energies as low as 60.0 MeV, which is significantly lower than the minimum energy used in experiment [14]. For E_{CM} at 59.5 MeV, an analysis of 2000 randomly selected initial orientations indicates that there is no pocket present in the ion-ion potential. Consequently, the fusion cross section is considered to be zero for $E_{CM} \leq 59.5$ MeV in the 3S-CMD calculation.

From Fig. 6, it has been observed that at higher energy levels, the variation in fusion cross-sections computed using the SBPM and 3S-CMD models is small. When energy levels decrease, the fusion cross-sections calculated from the 3S-CMD model show an enhancement compared to those obtained from the SBPM, where all dynamic effects are explicitly ignored. The shift from the SBPM calculations is clearly a result of the reorientation + vibrational effect occurring in the 3S-CMD model.

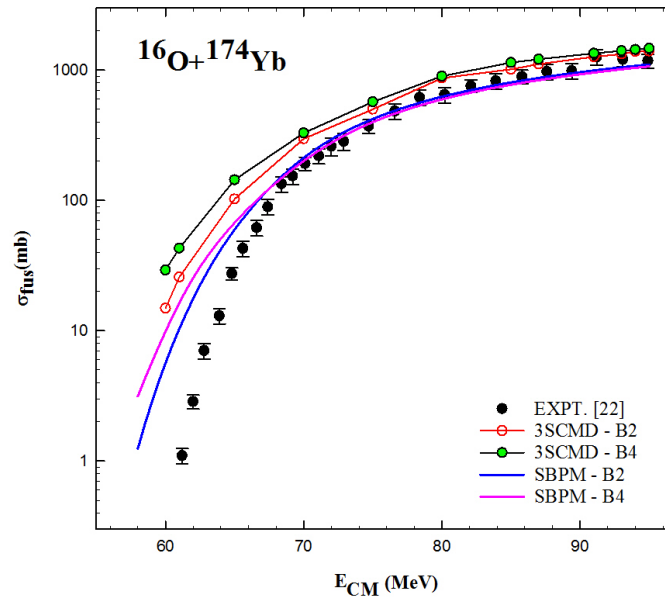


Figure 6. Comparison of fusion cross sections calculated for quadrupole and hexadecapole deformation using SBPM and 3S-CMD model with experimental fusion cross sections for $^{16}\text{O} + ^{174}\text{Yb}$ system.

Since the target nucleus (^{174}Yb) used in the above calculation is heavy and has principal moment of inertia components $I_1 = 3474.112 \text{ u fm}^2$; $I_2 = 3826.939 \text{ u fm}^2$ and $I_3 = 3902.096 \text{ u fm}^2$, the extent of reorientation is small as shown in Fig. 7. The principal moment of inertia components of projectile nucleus (^{16}O) are $I_1 = 59.182 \text{ u fm}^2$; $I_2 = 68.651 \text{ u fm}^2$ and $I_3 = 68.806 \text{ u fm}^2$. The evolution of these two nuclei begins at a distance of 2500 fm, influenced by the Coulomb field of each other. The reorientation of the deformed ^{174}Yb nucleus at different collision energies is shown in Fig. 7, where the initial orientation angle is set at $\beta_0 = 0$, $\alpha_0 = 0$, $\gamma_0 = 0$ and $R_{\text{in}} = 2500 \text{ fm}$. This figure clearly indicates that the extent

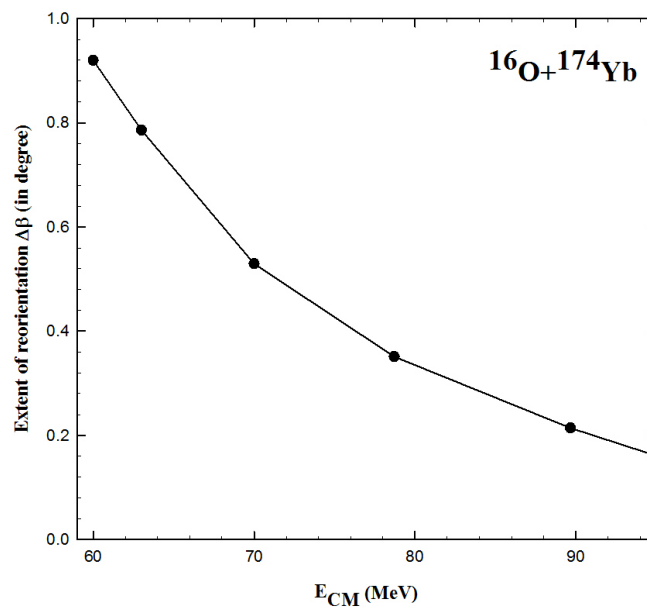


Figure 7. Extent of reorientation $\Delta\beta$ at the barrier top against E_{CM} for $^{16}\text{O} + ^{174}\text{Yb}$ system.

of reorientation of the ^{174}Yb nucleus is less than 1° , even at the lowest energy of 60 MeV. The reorientation value of the deformed nucleus, ^{174}Yb , is too small to have a significant effect on the fusion cross-sections. Therefore, the enhancement in fusion cross sections in 3S-CMD model with SBPM model is due to the vibrational excitations which occur close to the barrier or inside of it.

4. CONCLUSIONS

The above study explains the effect of hexadecapole deformation (β_4) on fusion cross sections of different systems in heavy ion collision. Although quadrupole deformation (β_2) is the most commonly examined type of deformation in nuclear fusion reactions, hexadecapole deformation (β_4) can also significantly influence fusion cross sections, particularly in systems where higher-order deformations play a crucial role.

From the above study, it is clear that the fusion cross section calculated with the quadrupole deformation shows smaller enhancement at lower energies than the fusion cross sections calculated with the hexadecapole deformation with the experiment. At higher energies heavy mass nucleus system (i.e., $^{16}\text{O} + ^{174}\text{Yb}$) gives better agreement with experiment than the medium-heavy mass nucleus system (i.e., $^{16}\text{O} + ^{154}\text{Sm}$).

ORCID

📧 Jignasha Patel, <https://orcid.org/0009-0008-1454-4283>; 📧 Vipul Katariya, <https://orcid.org/0009-0001-7215-8128>

APPENDIX A CALCULATION OF HEXADECAPOLE DEFORMATION (β_4)

The nuclear surface can be characterized by the radius vector \vec{R} in the direction (θ, ϕ) as given below [23],

$$R(\theta, \phi) = R_0 \left[1 + \sum_{\lambda=0}^{\infty} \sum_{\mu=-\lambda}^{\lambda} \alpha_{\lambda\mu} Y_{\mu}^{\lambda}(\theta, \phi) \right], \quad (6)$$

where R_0 is the radius of the spherical nucleus, and the terms containing $\alpha_{\lambda\mu}$ represent the expansion of any general function of the angles (θ, ϕ) in terms of the complete set of spherical harmonics $Y_{\mu}^{\lambda}(\theta, \phi)$. For the deformed partner, we shall restrict ourselves to only axially symmetric deformations of nucleus characterized by nuclear quadrupole and hexadecapole deformation parameters β_2 and β_4 respectively. In this case the nucleus can only rotate around an axis perpendicular to the symmetry axis. In terms of these, the radius of a deformed system is written as,

$$\begin{aligned} R(\theta) &= R_0 \left[1 + \beta_2 Y_2^0(\theta, \phi) + \beta_4 Y_4^0(\theta, \phi) \right] \\ &= R_0 \left[1 + \beta_2 \left(\frac{1}{4} \sqrt{\frac{5}{\pi}} (3\cos^2\theta - 1) \right) + \beta_4 \left(\frac{3}{16} \sqrt{\frac{1}{\pi}} (35\cos^4\theta - 30\cos^2\theta + 3) \right) \right], \end{aligned} \quad (7)$$

where,

R_0 in the present study is taken as rms radius of the nucleus.

$$Y_2^0(\theta, \phi) = \frac{1}{4} \sqrt{\frac{5}{\pi}} (3\cos^2\theta - 1)$$

$$Y_4^0(\theta, \phi) = \frac{3}{16} \sqrt{\frac{1}{\pi}} (35\cos^4\theta - 30\cos^2\theta + 3)$$

$R(\theta)$ is the magnitude of the radius vector of the nucleus at an angle θ with respect to the symmetry axis of the nucleus. Substituting $\theta = 90^\circ$ in the eq. (7), we get,

$$\begin{aligned} R(90) &= R_0 \left[1 - \beta_2 \left(\frac{1}{4} \sqrt{\frac{5}{\pi}} \right) + \beta_4 \left(\frac{3}{16} \sqrt{\frac{1}{\pi}} (3) \right) \right] \\ &= R_0 \left[1 - \beta_2 \left(\sqrt{\frac{5}{16\pi}} \right) + \beta_4 \left(\frac{9}{16} \sqrt{\frac{1}{\pi}} \right) \right] \end{aligned}$$

or

$$\begin{aligned} \frac{R(90)}{R_0} &= 1 - \beta_2 \left(\sqrt{\frac{5}{16\pi}} \right) + \beta_4 \left(\frac{9}{16} \sqrt{\frac{1}{\pi}} \right) \\ \beta_4 \left(\frac{9}{16} \sqrt{\frac{1}{\pi}} \right) &= \left[\frac{R(90)}{R_0} - 1 + \beta_2 \left(\sqrt{\frac{5}{16\pi}} \right) \right] \end{aligned}$$

which gives an expression for the hexadecapole deformation parameter β_4 as

$$\beta_4 = \left(\frac{16}{9} \sqrt{\pi} \right) \left[\frac{R(90)}{R_0} - 1 + \beta_2 \left(\sqrt{\frac{5}{16\pi}} \right) \right], \quad (8)$$

in terms of rms radius of the nucleus and $R(90^\circ)$ which is the length of the axes along the direction of any one of the principal axes perpendicular to the symmetry axis.

REFERENCES

- [1] A. Iwamoto, and P. Moller, Nucl. Phys. A, **605**, 334 (1996). [https://doi.org/10.1016/0375-9474\(96\)00155-8](https://doi.org/10.1016/0375-9474(96)00155-8)
- [2] R. K. Gupta, et al., Journal of Physics G: Nucl. Part. Phys. **31**, 631 (2005). [10.1088/0954-3899/31/7/009](https://doi.org/10.1088/0954-3899/31/7/009)
- [3] R. C. Lemmon, et al., Phys. Lett. B, **316**, 32 (1993). [https://doi.org/10.1016/0370-2693\(93\)90653-Y](https://doi.org/10.1016/0370-2693(93)90653-Y)
- [4] J.F. Niello, and C. H. Dasso, Lecture Notes in Physics **317**, 56-60 (2005). <https://link.springer.com/book/10.1007/3-540-50578-4>
- [5] H. Sharma, et al., The European Physical Journal A, **59**, 71 (2023). <https://link.springer.com/article/10.1140/epja/s10050-023-00981-1>
- [6] P. Moller, Nucl. Phys. A, **142**, 1 (1970). [https://doi.org/10.1016/0375-9474\(70\)90469-0](https://doi.org/10.1016/0375-9474(70)90469-0)
- [7] U. Gotz, et al., Nucl. Phys. A, **192**, 1 (1972). [https://doi.org/10.1016/0375-9474\(72\)90002-4](https://doi.org/10.1016/0375-9474(72)90002-4)
- [8] S. S. Godre, and Y. R. Waghmare, Phys. Rev. C, **36**, 1632 (1987). <https://doi.org/10.1103/PhysRevC.36.1632>
- [9] S. S. Godre, Pramana J. Phys. **82**, 879 (2014). <https://doi.org/10.1007/s12043-014-0741-6>
- [10] S. S. Godre, Nucl. Phys. A, **734**, E17 (2004). <https://doi.org/10.1016/j.nuclphysa.2004.03.009>
- [11] P. R. Desai, Ph.D. Thesis, "Effect of Coulomb reorientations on fusion crosssections and barrier distributions of some heavy-ion reactions," Veer Narmad South Gujarat University, Surat (2009).
- [12] I. B. Desai, and S. S. Godre, Proc. Int. Symp. on Nucl. Phys. **54**, 196 (2009). <https://www.sympnp.org/proceedings/54/A72.pdf>
- [13] S.S. Godre, and P.R. Desai, Proc. Symp. on Nucl. Phys. **53**, 341 (2008).
- [14] C. Simenel, et al., Phys. Rev. Lett. **93**, 102701 (2004). <https://doi.org/10.1103/PhysRevLett.93.102701>
- [15] S. E. Koonin, et al., Phys. Rev. C, **15**, 1359 (1977). <https://doi.org/10.1103/PhysRevC.15.1359>
- [16] R. Birkelund, et al., Phys. Rep. **56**, 107 (1979). [https://doi.org/10.1016/0370-1573\(79\)90093-0](https://doi.org/10.1016/0370-1573(79)90093-0)
- [17] N. I. Chauhan, "A Study of near-barrier fusion of some heavy-ion collisions using coupled-channel calculation," M. Phil. Dissertation, Veer Narmad South Gujarat University, Surat (2012).
- [18] C. Y. Wong, Phys. Rev. Lett. **31**, 766 (1973). <https://doi.org/10.1103/PhysRevLett.31.766>
- [19] P. R. Desai, and S. S. Godre, Eur. Phys. J. A, **47**, 146 (2011). <https://doi.org/10.1140/epja/i2011-11146-8>
- [20] S. S. Godre, and Y. R. Waghmare, Phys. Rev. C, **36**, 1632 (1987). <https://doi.org/10.1103/PhysRevC.36.1632>
- [21] J. R. Leigh, et al., Phys. Rev. C, **47**, R437 (1993). <https://doi.org/10.1103/PhysRevC.47.R437>
- [22] T. Rajbongshi, et al., Phys. Rev. C, **93**, 054622 (2016). <https://doi.org/10.1103/PhysRevC.93.054622>
- [23] M. K. Pal, *Theory of Nuclear Structure*, 382, (Allied East-West press Pvt. Ltd., 1982).

ВПЛИВ ГЕКСАДЕКАПОЛЬНОЇ ДЕФОРМАЦІЇ НА ПОПЕРЕЧНІ ПЕРЕРІЗИ СИНТЕЗУ ДЕЯКИХ СФЕРИЧНИХ + ДЕФОРМОВАНИХ СИСТЕМ У МОДЕЛІ 3S-CMDДжігнаша Пател¹, Віпул Катарія²¹Вір Нармад, Університет Південного Гуджарату, Сураат - 395007, Гуджарат, Індія²Кафедра фізики, Науковий коледж Атмананд Сарасваті, Сураат - 395006, Гуджарат, Індія

Вплив квадрупольної деформації (β_2) на синтез важких іонів є добре відомим явищем. Окрім впливу квадрупольної деформації (β_2), потенційний вплив гексадекапольної деформації (β_4) на суббар'єрний синтез був предметом частих обговорень. Нещодавно було проведено теоретичний аналіз для вивчення впливу гексадекапольних деформацій (β_4) з використанням спрощеного коду зв'язаних каналів SCFUS, який враховує статичні деформації. У цьому дослідженні ми аналізуємо вплив β_4 цільового ядра на перерізи синтезу в рамках моделі 3S-CMD. Для цього ми обрали реакції $^{16}\text{O} + ^{154}\text{Sm}$ та $^{16}\text{O} + ^{174}\text{Yb}$. У цьому дослідженні перерізи синтезу також розраховано за допомогою моделі SBPM. Розраховані перерізи синтезу за допомогою моделі 3S-CMD та SBPM порівнюються між собою, а також з експериментом.

Ключові слова: деформовані ядра; квадруполь; гексадекаполь; перерізи синтезу; класичні мікроскопічні підходи; реакції важких іонів